

Fusion and stability of colliding atomic nuclei, atomic clusters, and liquid droplets

R. Schmidt* and H. O. Lutz

Fakultät für Physik, Universität Bielefeld, 4800 Bielefeld 1, Germany

(Received 23 September 1991)

We propose a simple stability condition of collisionally fused aggregates. The model provides a description of the fusion cross section for colliding nuclei, clusters, and liquid droplets at large energies.

PACS number(s): 36.40.+d, 25.70.-z

Concepts that are useful in different fields of research can be pleasing and stimulating as well. Recent examples may, e.g., be found in the study of atomic clusters. It is now well established that the understanding of some of their *structural* properties is greatly aided by application of concepts that have also been used in nuclear physics [1]. It is therefore tempting to look for other common concepts that may shed further light on their *dynamical* behavior also. To this end, we have recently begun a systematic theoretical study on general aspects of cluster-cluster collisions [2,3]. Aside from characteristic differences, many analogies to nuclear heavy-ion collisions (HIC) are found, in particular, the close correspondence of dominant reaction channels: quasi-elastic, deep inelastic, and fusion. An important question in this context is the stability of the rotating intermediate complex, which limits the fusion cross section [3] and which represents also a long-standing problem in nuclear HIC (see, e.g., Ref. [4]).

In this article we treat, on the basis of a simple model, the stability of collisionally fused rotating aggregates (nuclei, droplets, and clusters) and the related high-energy fusion cross sections. In doing so, we apply the concept of a maximum angular momentum above which the systems become unstable against centrifugal fragmentation.

For the purpose of further arguments we briefly sketch the gross behavior of the complete fusion (or fusion-evaporation) cross section σ_{CF} in nuclear HIC, and briefly summarize its interpretation. At low bombarding energies, above the Coulomb barrier for fusion, the energy dependence of $\sigma_{CF}(E)$ can be well understood within the so-called "critical-distance concept" [5,6]. In this model, fusion is assumed to take place with unit probability if the approaching nuclei reach a critical distance R_C between their centers in the effective interaction potential of the entrance channel. The critical-distance model can be regarded as the specific "nuclear" realization of the simplest geometrical reaction model; it has also been applied in other fields (e.g., chemical-reaction theory) and serves as a useful first-order approximation in the development of more refined reaction theories. According to the peculiarities of the nuclear interaction potential, the critical-distance concept yields the well-known behavior of the low-energy fusion cross section in terms of (in general) two energy regions, in which the fusion cross section is limited by the potential values at the Coulomb barrier and at the critical distance, respectively. Beyond a cer-

tain energy E_{cr} , however, angular momenta l occur which are too great to allow formation of a stable rotating complex. The high-energy complete fusion cross section then becomes (for a recent discussion see Ref. [4])

$$\sigma_{CF} \approx \pi l_{cr}^2 / 2\mu E \quad (1)$$

with l_{cr} a maximum allowed energy-independent angular momentum. By fitting the energy dependence of available experimental high-energy fusion-evaporation cross sections to Eq. (1), we have extracted l_{cr} (Fig. 1). It is interesting to note that (in contrast to earlier expectations [17]) l_{cr} is well below the angular momentum for which the *fission* barrier vanishes (cf. Fig. 1). So far, no deeper justification of l_{cr} has been given. However, a clue for a better understanding of macroscopic aspects of nuclear HIC may be provided by recent experiments with colliding liquid droplets [18,19].

An important problem in aerosol physics, the fusion of droplets with diameters typically around 100 μm , has been studied recently [18,19]. In the experiments the impact parameter for fusion b_{CF} (i.e., $\sigma_{CF} = \pi b_{CF}^2$) versus impact velocity v is measured. *The comparison with HIC reveals the close correspondence of the collision dynamics of both systems:* At low impact velocities, b_{CF} is constant and given by the sum of the radii of the colliding droplets, $b_{CF} = R_{12} = R_1 + R_2$ [18,19]. It therefore represents the simplest (trivial) case of a system where the critical-distance concept applies, namely, for noninteracting uncharged spheres with $R_C = R_{12}$. At high impact velocities, $b_{CF}(v)$ decreases to good approximation with $1/v$, again equivalently to nuclear HIC [i.e., Eq. (1)]; therefore, in terms of a critical angular momentum, b_{CF} can be written (in dimensionless form) as

$$\frac{b_{CF}}{R_{12}} = \frac{l_{cr}}{R_{12}\mu} \frac{1}{v} \equiv \frac{v_{cr}}{v}, \quad v \geq v_{cr}. \quad (2)$$

In contrast to nuclei (and atomic clusters [3]) where the critical energy above which Eq. (1) becomes valid depends on the potential energy at R_C , in the case of (noninteracting) droplets l_{cr} directly determines $v_{cr} = l_{cr} / \mu R_{12}$ in Eq. (2). A typical example of experimental results at $v \geq v_{cr}$ is shown in Fig. 2.

Such systems can be viewed directly by optical techniques [18]. Their behavior suggests the following picture for the course of the collision in terms of an idealized

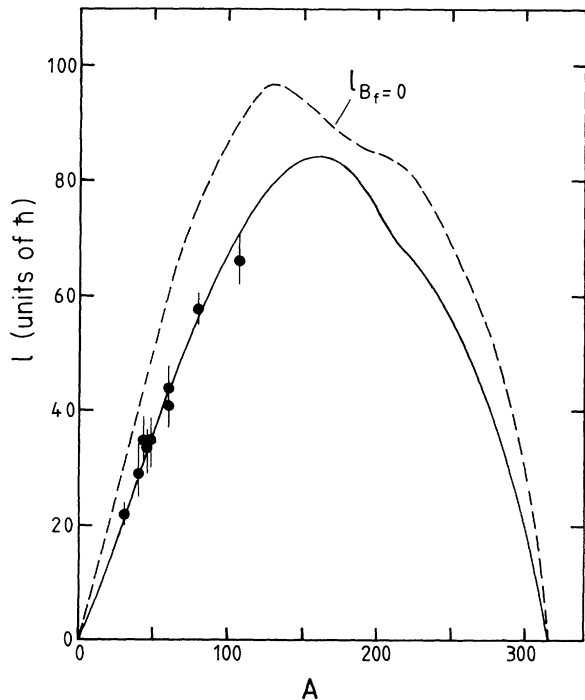


FIG. 1. Experimental (points) and calculated (solid line) critical angular momenta l_{cr} for fusion in HIC as function of the total mass number A . For comparison, the angular momenta for vanishing fusion barriers $l_{B_f=0}$ (dashed line) taken from Ref. [17] are presented. The experimental points correspond to the following collision systems: $^{12}\text{C}+^{18}\text{O}$, $^{13}\text{C}+^{17}\text{O}$ (one point in the figure) taken from Ref. [7]; $^{12}\text{C}+^{27}\text{Al}$, Ref. [8]; $^{16}\text{O}+^{27}\text{Al}$, Refs. [9–11]; $^{20}\text{Ne}+^{26}\text{Mg}$, Ref. [12]; $^{20}\text{Ne}+^{27}\text{Al}$, Ref. [13]; $^{19}\text{F}+^{40}\text{Ca}$, Ref. [14]; $^{32}\text{S}+^{27}\text{Al}$, Refs. [9,14]; $^{40}\text{Ca}+^{40}\text{Ca}$, Ref. [15]; $^{32}\text{S}+^{76}\text{Ge}$, Ref. [16].

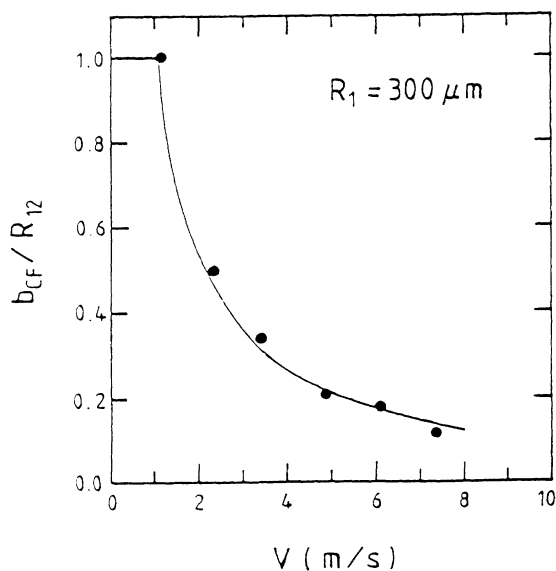


FIG. 2. Experimental [19] and calculated (line) impact parameter for fusion b_{CF}/R_{12} vs impact velocity v for water droplets of equal radii $R_1 = R_2 = 300 \mu\text{m}$.

trajectory in the potential landscape of a rigid rotator whose deformation energy we express by the surface and Coulomb energies: upon contact, the steep gradient of the surface energy rapidly pulls the two-sphere configuration towards a nearly spherical rotating shape; all available radial kinetic energy is dissipated into heat. At large angular momenta, the compound then undergoes slow and weakly damped shape oscillations along the fission path in the multidimensional *shallow* effective potential. The optical imaging of droplet collisions strongly supports this view; in particular, the rapid collapse to a near-spherical rotating compound and the ensuing slow, weakly damped shape oscillations can be clearly discerned. In this picture, the compound is stable if the total collective (rotational and potential) energy of the spherical complex (0) does not exceed the fission barrier located at the saddle (S), i.e., l_{cr} is fixed by

$$E_S^{\text{surf}} + E_S^{\text{Coul}} + l_{cr}^2/2I_S = E_0^{\text{surf}} + E_0^{\text{Coul}} + l_{cr}^2/2I_0 \quad (3)$$

with E^{surf} and E^{Coul} the surface and Coulomb energy parts of the potential energy, and I the moment of inertia. We use the charge (“fissility”) and angular momenta in terms of dimensionless quantities

$$x \equiv E_0^{\text{Coul}}/2E_0^{\text{surf}}, \quad y \equiv l^2/2I_0E_0^{\text{surf}}. \quad (4)$$

For liquid uniformly charged masses of surface tension σ the energies of the saddle shapes have been calculated [17]. For simplicity, we parametrize the results (Fig. 12 in Ref. [17]), thereby requiring our stability condition Eq. (3) to be observed. This yields

$$y_{cr}(x) = \begin{cases} 0.38 - 0.4857x, & 0 \leq x \leq 0.7 \\ 0.3289(1-x)^{1.75}, & 0.7 \leq x \leq 1. \end{cases} \quad (5)$$

Thus $l_{cr}^2 = 2I_0E_0^{\text{surf}}y_{cr}(x)$ with $I_0 = 2MR_0^2/5$ and $E_0^{\text{surf}} = 4\pi\sigma R_0^2$ (M the total mass, R_0 the radius of the spherical compound). Any effect of the temperature increase on σ (induced by the dissipation of kinetic energy) remains negligibly small in the systems discussed below.

Application of the model. We shall now specify these general considerations for the three cases considered, namely nuclear, droplet, and cluster collisions, and compare the results to available experimental data.

(i) *Atomic nuclei.* Using standard parameters for the surface tension σ of nuclei [17] the fissility of a system with total charge Z and mass number A is $x = 0.01965Z^2/(1-1.7826c^2)A$ with $c = (A-2Z)/A$; with this we obtain in units of \hbar

$$l_{cr} = [0.5195(1-1.7826c^2)A^{7/3}y_{cr}(x)]^{1/2}\hbar. \quad (6)$$

This result is plotted in Fig. 1; Z has been taken in the valley of β stability, $(A-2Z) = 0.4A^2/(200+A)$. Evidently, Eq. (6) compares quite favorably with the experimental l_{cr} values.

(ii) *Macroscopic droplets.* Since the Coulomb energy is insignificant (unless Z is very large), $x \approx 0$ and $y_{cr} \approx 0.38$ [cf. Eqs. (4) and (5)]. Typically, $l_{cr} \gtrsim 10^{20}\hbar$ in this case. Thus for macroscopic systems, it is more convenient to use v_{cr} instead of l_{cr} ,

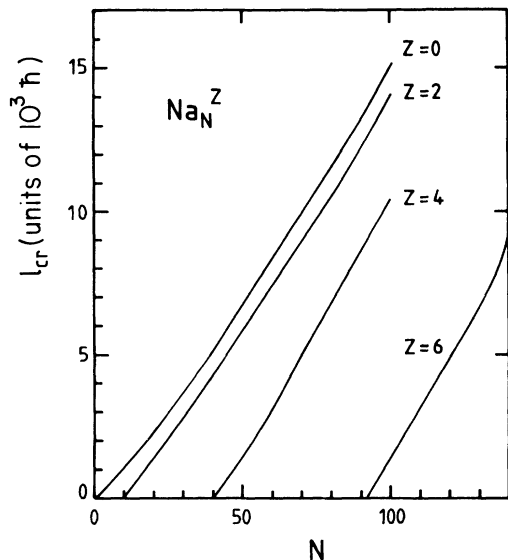


FIG. 3. Calculated critical angular momenta for fusion l_{cr} (in units of $10^3 \hbar$) for sodium clusters Na_N^Z with N atoms and charge number Z as function of N .

$$v_{cr} = \left[\frac{12}{5} \frac{(R_1^3 + R_2^3)^{13/3}}{R_1^6 R_2^6 (R_1 + R_2)^2} \frac{\sigma}{\rho} y_{cr} \right]^{1/2} \quad (7)$$

with ρ the density of the liquid. For water droplets ($\rho = 1 \text{ g/cm}^3$; $\sigma = 73 \text{ dyn/cm}$) with equal radii $R_1 = R_2 = 300 \text{ } \mu\text{m}$ this yields a critical velocity of $v_{cr} \approx 1.1 \text{ m/s}$, and the calculated relative impact parameter for fusion b_{CF}/R_{12} versus v is plotted in Fig. 2. The results compare favorably with the depicted experimental example.

(iii) *Atomic clusters.* For atomic clusters, characterized by the Wigner-Seitz radius r_s and the number of atoms N with atomic weight A_{rel} , one obtains (again in units of \hbar)

$$l_{cr} = [0.01177 A_{rel} r_s^4 \sigma N^{7/3} y_{cr}(x)]^{1/2} \hbar, \quad (8)$$

where r_s should be taken in atomic units and σ in dyn/cm. x and $y_{cr}(x)$ depend, of course, on the nature of the charge distribution in the cluster. For neutral clusters, $x = 0$ and thus $y_{cr} = 0.38$; for uniformly charged clusters, y_{cr} is given by Eq. (5). Surface charged (metallic) clusters exhibit other saddle shapes and energies (although the critical sizes against Coulomb explosion are correctly obtained with $x = 1$; a detailed analysis will be given elsewhere [20]). As a lower limit estimate for surface charged cluster, i.e., $x = 3.098 \times 10^4 (Z^2 / N r_s^3 \sigma)$ [r_s, σ in the same units as in Eq. (8)], we use Eq. (5) for $y_{cr}(x)$. In Fig. 3, l_{cr} values calculated for fused Na_N^Z clusters ($r_s = 3.93 \text{ a.u.}$, $\sigma = 200 \text{ dyn/cm}$, $A_{rel} = 23.0$) are displayed. They are typically in the range of several thousand units of \hbar ; starting from the critical sizes against Coulomb explosion, they rise steeply with N and

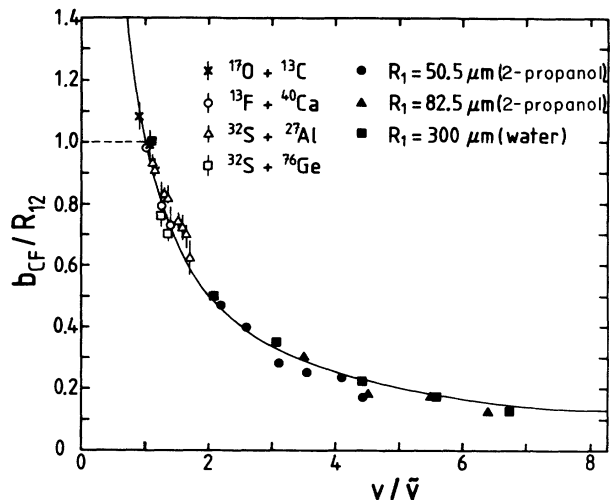


FIG. 4. Universal scaling of the dimensionless impact parameter for fusion b_{CF}/R_{12} vs impact velocity v/\bar{v} (solid line) as compared to experimental data for different (symmetric) droplet collision [18,19] (full points) and nuclear HIC [7,14,9,16] (points with error bars).

depend strongly on Z . No experimental data are available yet although it may be noted that first experiments on cluster-cluster collisions are in progress [21]. A detailed theoretical discussion of the expected fusion cross-section behavior as a function of cluster size, charge, and impact energy is planned to be given in a future paper [3].

Universal scaling. With $\bar{v} = l_{cr}/\mu R_{12}$ and the dimensionless (scaled) presentation of b_{CF}/R_{12} as a function of v/\bar{v} one can merge experimental data of different droplet collisions as well as HIC into one plot which according to Eq. (2) should follow the same universal scaling law (Fig. 4). For HIC, we commonly put $R_{12} = R_C = 1.0 \text{ fm} (A_1^{1/3} + A_2^{1/3})$ [5,6]; tabulated values of $\rho = 0.7853 \text{ g/cm}^3$ and $\sigma = 21.4 \text{ dyn/cm}$ for 2-propanol-droplet collisions are used. The calculated critical velocities for $R_1 = R_2 = 50.5$ and $82.5 \text{ } \mu\text{m}$ are $v_{cr} = 1.57$ and 1.23 m/s , respectively. Apparently, the scaling law for fusion (solid line in Fig. 4) has an impressively wide range of validity; note that collision dimensions and critical angular momenta differ by more than 10 and 20 orders of magnitude, respectively. For droplets, where $\bar{v} \equiv v_{cr}$, b_{CF}/R_{12} is unity at $v/\bar{v} \leq 1$ (dashed line in Fig. 4). In contrast for nuclei, b_{CF}/R_{12} can exceed unity in this velocity range due to finite negative values of the potential energy at contact.

Helpful discussions with Dr. R. W. Hasse are gratefully acknowledged. We especially thank Dr. G. Brenn for providing us with actualized experimental data of collisions between 2-propanol droplets. This work has been supported by the Deutsche Forschungsgemeinschaft.

*Permanent address: Institut für Theoretische Physik, Technische Universität Dresden, Germany.

[1] Cf., e.g., *Proceedings of the 88th WE-Heraeus Seminar on Nuclear Physics Concepts in Atomic Cluster Physics*, edited

by R. Schmidt, H. O. Lutz, and R. Dreizler, Lecture Notes in Physics (Springer, Heidelberg, in press).

[2] R. Schmidt, G. Seifert, and H. O. Lutz, *Phys. Lett. A* **158**, 231 (1991); G. Seifert, R. Schmidt, and H. O. Lutz, *ibid.*

- 158, 237 (1991).
- [3] R. Schmidt and H. O. Lutz (unpublished).
- [4] G. Doukellis, *Phys. Rev. C* **37**, 2233 (1988).
- [5] J. Galin, D. Guerreau, M. Lefort, and X. Tarrago, *Phys. Rev. C* **9**, 1018 (1974).
- [6] D. Glas and U. Mosel, *Phys. Rev. C* **10**, 2620 (1974); *Nucl. Phys.* **A237**, 429 (1975); **A264**, 268 (1976).
- [7] B. Heusch *et al.*, *Phys. Rev. C* **26**, 542 (1982).
- [8] R. R. Betts, W. A. Lanford, M. H. Mortensen, and R. L. White, Argonne National Laboratory Report No. ANL-Phys. 76-2 (1976) p. 443 (unpublished); R. R. Betts [private communication quoted in J. R. Birkelund *et al.* *Phys. Rev. C* **56**, 107 (1979)].
- [9] R. L. Kozub *et al.*, *Phys. Rev. C* **11**, 1497 (1975).
- [10] B. Back *et al.*, *Nucl. Phys.* **A285**, 317 (1977).
- [11] R. Rascher, W. F. J. Müller, and K. P. Lieb, *Phys. Rev. C* **20**, 1028 (1979).
- [12] H. Lehr *et al.*, *Nucl. Phys.* **A415**, 149 (1984).
- [13] H. Morgenstern *et al.*, *Z. Phys. A* **113**, 39 (1983).
- [14] G. Rosner *et al.*, *Phys. Lett.* **150B**, 87 (1985).
- [15] H. Doubre *et al.*, *Phys. Lett.* **73B**, 135 (1978).
- [16] G. Guillaume *et al.*, *Phys. Rev. C* **26**, 2458 (1982).
- [17] S. Cohen, F. Plasil, and W. J. Swiatecki, *Ann. Phys. (N.Y.)* **82**, 557 (1974).
- [18] G. Brenn and A. Frohn, *Exp. Fluids* **7**, 441 (1989); *Spektrum Wissenschaft* **12**, 116 (1990); (private communication).
- [19] J. R. Adam, N. R. Lindblad, and C. D. Hendricks, *J. Appl. Phys.* **39**, 5173 (1968).
- [20] R. W. Hasse, R. Schmidt, and H. O. Lutz (unpublished).
- [21] E. E. B. Campbell, A. Hielscher, R. Ehlich, and I. V. Hertel, in Ref. [1].